

# Comparative analysis of experimental and modelling of gas-solid flow hydrodynamics: Effect of friction and interparticle cohesion forces

Yassir Makkawi<sup>1</sup>, Phillip Wright<sup>2</sup> and Raffaella Ocone<sup>1</sup>

1. Heriot-Watt University, School of Engineering and Physical Sciences, Department of Chemical Engineering, Edinburgh, EH14 4AS, UK

2. The University of Sheffield, Biological & Environmental Systems Group, Department of Chemical and Process Engineering, Mappin Street, Sheffield, S1 3JD, UK

## 1. Introduction

For many years, solid-gas flow has been simulated with great success using the two fluid model based on kinetic theory (Huilin et al., 2003). However, recent work on experimental validation of traditional CFD models has shown poor simulation for dense flow such as bubbling bed. Several researchers have noted that the kinetic theory prediction shows an overestimated bubbling bed expansion when compared to experimental data (Mckeen and Pugsley 2003; Ferschneider and Mega, 1996). They attributed this to the fact that most of the available CFD models only account for the solid collisional/viscous forces but do not adequately represent or completely ignore the other possible contact forces such as the interparticle cohesion or frictional forces,

In this study further investigations in this issue have been carried out using experimental data obtained in a bubbling bed using Electrical Capacitance Tomography (ECT). The experimental data has been compared to the time dependent hydrodynamic predictions of MFIX simulation code. In order to investigate the effect of cohesion and frictional forces on the hydrodynamic features in general granular flow, a parametric sensitivity analysis has been carried out using a simple one-dimensional fully developed flow model (ocone et al., 1993). A continuous frictional term, applicable to dilute-intermediate-dense flow, and a cohesive term applicable to group A/B particles, has been implemented and its effect on the flow behaviour has been discussed in the context of the experimental-MFIX comparison.

## 2. Experimental:

The ECT is a sensitive scientific instrument consisting mainly of electrical capacitance sensors, data acquisition module and a computer. For two-phase mixture, such as gas-solid flow, the ECT can measure the spatial distribution of the composite permittivity of the two materials inside a confining volume. Then from this permittivity data, it is possible to obtain the distribution of the relative distribution of the two components over the cross-section of the bed. Further details on the ECT system and calibration procedure can be found in Makkawi et. al (2004) and PTL release notes (Process Tomography Ltd, Wilmslow, UK).

The experiments were carried out in a cold conventional bubbling bed, consisting of cast acrylic tube allowing for direct visual observation. A perforated gas distributor was placed 30 cm above the bottom of the column. Air at ambient temperature was introduced to the bottom of the column from a main air compressor. The experimental set-up is shown in Fig. 1 and the experimental operating conditions are summarized in Table 1. Tomography measurements were taken at two different levels above the distributor plate,

and at various gas velocities. Further experimental descriptions and measuring procedure can be found in details in [Makkawi \(2004\)](#).

**Table 1. Experimental conditions.**

| Experimental unit | Operating Conditions  |
|-------------------|---|
| Column            | Dia. = 0.138 m, height = 1.5 m, material: Plexiglas   |
| Distributor       | Perforated PVC; 150 holes of 2 mm dia.  |
| Particles         | Group A/B $d_p = 90 \mu\text{m}$ , $\rho_p = 2500 \text{ kg/m}^3$<br>Group B $d_p = 350 \mu\text{m}$ , $\rho_p = 2500 \text{ kg/m}^3$     |
| Fluidizing Gas    | Material: glass ballotini<br>Air at ambient condition   |
| Static bed height | 13.8 cm   |
| Measuring level   | Level 1: Average between 0 - 3.8 cm, above distributor<br>Level 2: average between 3.8 - 5.7 cm, above distributor                        |
| ECT system        | Twin plane, 8 electrodes with guards<br>Sensor length: 3.8 cm, guard height: 7.6 cm<br>Data capture rate: 100 Hz<br>Experiment span: 80 s |

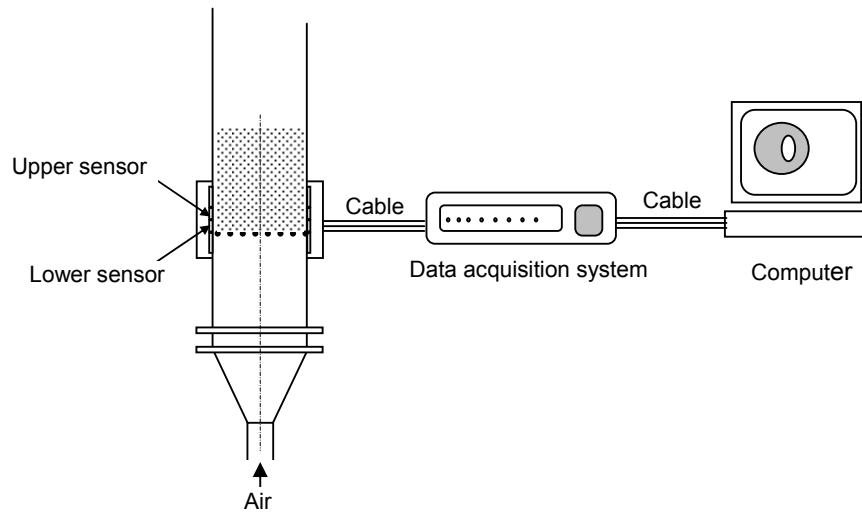


**Fig. 1. Experimental set up**

### 3. Mfix model equations

Mfix is abbreviation for the name “Multiphase Flow with Interphase eXchanges”. It is an open source Fortran code developed by Morgantown energy centre, part of the US department of energy. It is a general-purpose hydrodynamic model for fluid solid flow that gives time-dependent information (unsteady) for the pressure, velocity, temperature and concentration in a contained vessel.

For non-reacting isothermal solid-gas flow the model equations are given by:

$$\text{Solid- gas continuity equation: } \frac{\partial}{\partial t} (\epsilon_i \rho_i) + \nabla \cdot (\epsilon_i \rho_i u_i) = 0 \quad (i= \text{gas, solids}) \quad (1)$$

$$\text{Gas momentum: } \frac{\partial}{\partial t} (\epsilon_g \rho_g u_g) + \nabla \cdot (\epsilon_g \rho_g u_g u_g) = \nabla \cdot \bar{\bar{\tau}}_g + \epsilon_g \rho_g g + \beta(u_s - u_g) - \epsilon_g \nabla P_g \quad (2)$$

$$\text{Solid momentum: } \frac{\partial}{\partial t} (\epsilon_s \rho_s u_s) + \nabla \cdot (\epsilon_s \rho_s u_s u_s) = \nabla \cdot \bar{\bar{S}}_s + \epsilon_s \rho_s g + \beta(u_s - u_g) - \epsilon_s \nabla P_g \quad (3)$$

The MFIx code employs a simplified algebraic expression for the granular temperature obtained from the energy equation of [Lun et al. \(1984\)](#). For more details on the granular temperature equation and other closure equations the reader is referred to [Syamlal et al. \(1993\)](#) and MFIx document available at the open web [www.mfix.org](http://www.mfix.org).

The gas-solid drag model is given by the continuous formula of [Gibilaro et al. \(1985\)](#) given by:

$$\beta = \left( \frac{17.3}{\text{Re}_p} + 0.336 \right) \frac{\rho_g |u_s - u_g|}{d_p} \varepsilon_s \varepsilon_g^{-2.8} \quad (5)$$

This equation is assumed to give continuous values of  $\beta$  over all ranges of solid volume fraction.

At high solid fraction, frictional stresses become dominant over the kinetic stress (collisional/viscous) due to particle-particle contact. The radial frictional stress is given by [Jenike, 1978](#)

$$N_{f,yy} = \begin{cases} 10^{25} (\varepsilon_s - \varepsilon_{s,critical})^{10} & \text{if } \varepsilon_s > \varepsilon_{s,critical} \\ 0 & \text{if } \varepsilon_s \leq \varepsilon_{s,critical} \end{cases} \quad (6)$$

where  $\varepsilon_{s-critical} = 0.59$  is the critical solid fraction at which the frictional force starts to take place. The frictional shear,  $N_{f,xy}$ , is related to the solid frictional pressure  $N_{f,yy}$  by using the linear law of [Coulomb \(1776\)](#). This is given by:

$$N_{f,xy} = \frac{N_{f,yy} \overline{D} \sin \phi}{\sqrt{I_{2D}}} \quad (7)$$

where  $\overline{D}$  and  $I_{2D}$  are the strain rate and second deviator of the strain rate tensor respectively.

#### 4. Comparison of MFIx prediction with ECT data:

In order to compare predictions with experimental data, the MFIx simulation was carried out using exactly the same dimensions and material specifications used in the experimental part (see [Table 1](#)). The parameters used in the simulation are shown in [Table 2](#). Other model parameters are available in MFIx documents.

**Table 2. Parameters used for the MFIx simulation**

|   |  |
|---|--|
| Gas density, $\rho_g$                                   | 1.24 (kg.m <sup>-3</sup> )                                     |
| Molecular gas viscosity, $\mu_g$                        | 0.18 x 10 <sup>-4</sup> (kg.m <sup>-1</sup> .s <sup>-1</sup> ) |
| Particle-particle restitution coefficient, $e_p$        | 0.95 (-)   |
| Particle-wall restitution coefficient, $e_w$            | 0.99 (-)   |
| Internal angle of friction, $\phi$                      | 0.5 (degrees)  |
| Maximum allowable solid fraction, $\varepsilon_{s,max}$ | 0.65 (-)   |
| Critical solid fraction, $\varepsilon_{s,critical}$     | 0.59 (-)   |
| Mesh size   | 1.0 cm   |
| Simulation time   | 30 seconds   |

Fig.2 shows a comparison between the simulation and experimental solid fraction profile for Group B particles. The simulation using the original MFIX drag model of Syamlal (1993) and Gibilaro et al. (1985) are reasonably comparable with the experimental data.

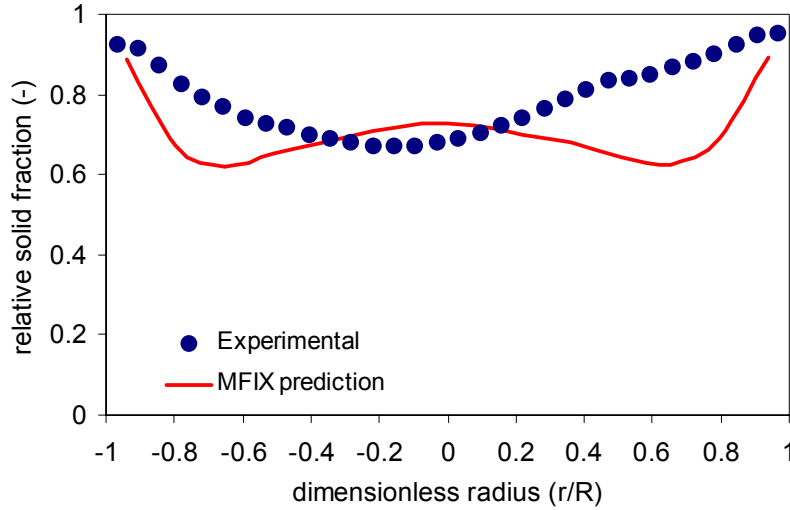


Fig. 2. Experimental and predicted solid fraction profile for Group B particles at  $U = 0.53$  m/s.

Fig. 3 shows the concept applied for estimating the bubble rise velocity as illustrated in a typical time series data of solid fraction fluctuation. The time lag,  $\Delta t$ , between the bubble peaks (lower solid fraction) detected at two different levels separated by a distance  $\Delta x$ , gives the instantaneous bubble velocity as follows:

$$u_b = \frac{\Delta x}{\Delta t} \quad (8)$$

and hence, the time-averaged bubble velocity  $\Delta x$ , is given by:

$$U_b = \frac{1}{n_b} \sum_{i=0}^{i=n_b} u_{b,i} \quad (9)$$

where  $n_b$  is the total number of bubbles detected in a specific time interval.

In a similar approach, the time-averaged bubble flow rate is given by:

$$Q_b = \frac{1}{n_b} \sum_{i=0}^{i=n_b} q_{b,i} \quad (10)$$

where  $q_b$  is the instantaneous bubble flow rate given as function of the bed cross-sectional area,  $A$  and the bubble velocity,  $u_b$ , such that

$$q_b = Au_b \varepsilon_b \quad (11)$$

where the bubble fraction,  $\varepsilon_b$ , given in terms of the relative solid fraction by  $\varepsilon_b = 1 - p$  ( $p$  varies between 0 and 1).

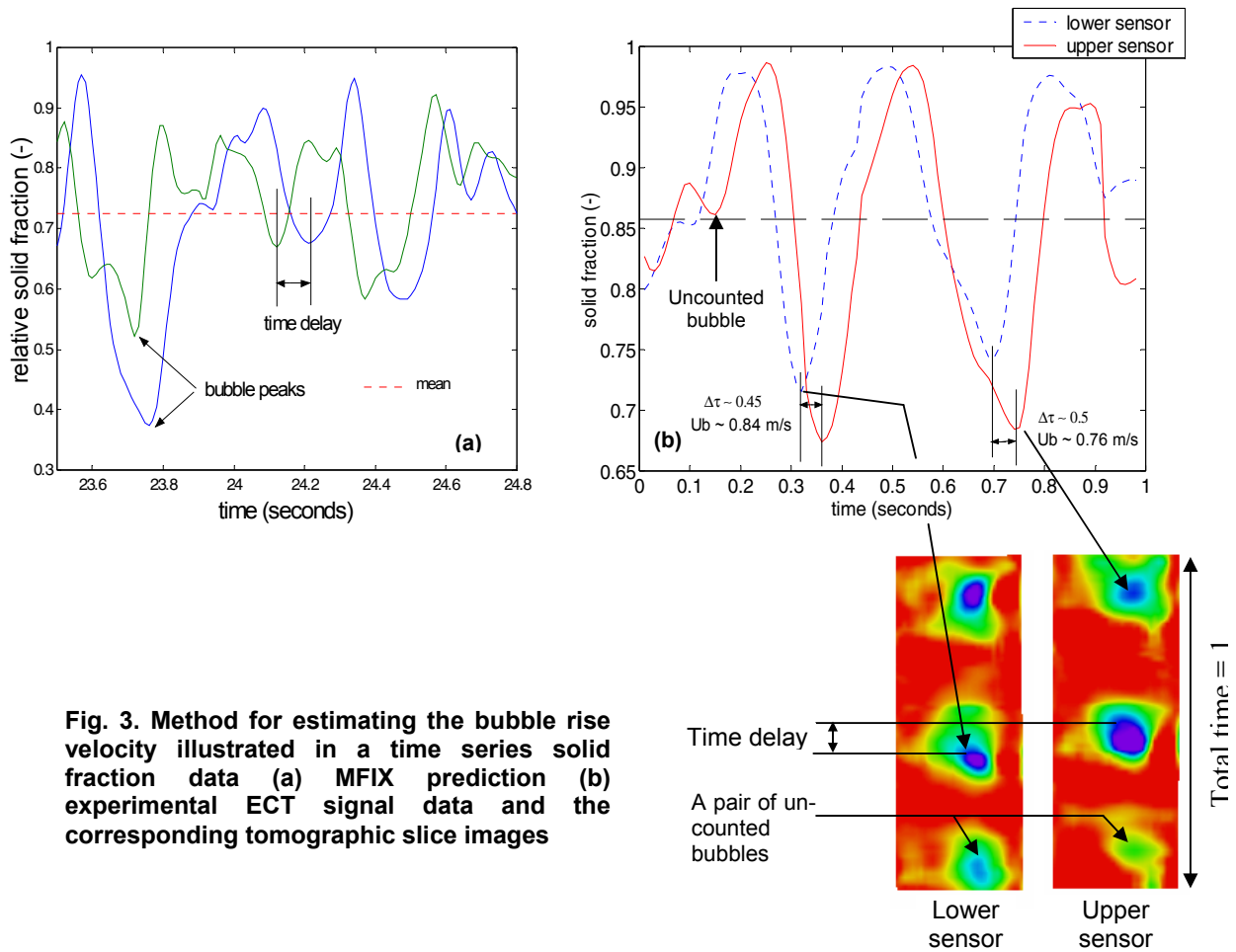


**Fig. 3. Method for estimating the bubble rise velocity illustrated in a time series solid fraction data (a) MFIX prediction (b) experimental ECT signal data and the corresponding tomographic slice images**

Table 3 shows the experimental and predicted bubble characteristics for Group B particles estimated at a superficial gas velocity of  $U = 0.53$  m/s. The bubble frequency was estimated from the time-series data of solid fraction fluctuation using the power spectra density analysis as shown in Fig. 4. It is clear here the model can predict the hydrodynamic feature of the bed with a high degree of accuracy. However, the prediction starts to deviate from the experimental data as the gas velocity increases, this is demonstrated in the cross-sectional solid fraction against the superficial gas velocity shown in Fig. 5, which indicates a clear overexpansion. The poor performance of MFIX at high gas velocity in this case can be attributed to the fact that in the MFIX formulations, the frictional stress are assumed negligible at relatively low solid fraction ( $\varepsilon_s < 0.59$ ). We believed that in a bubbling bed, the particle-particle friction is of significant importance and must be taken into consideration in order to have accurate predictions. This view shall be verified in the next Sections 5.2.

**Fig. 3. Experimental and predicted bubble characteristics in a bed of Group B at  $U = 0.53$  m/s.**

|                                      | Experimental | Mfix prediction |
|--------------------------------------|--------------|-----------------|
| Bubble frequency (Hz)                | 2.8          | 2.9             |
| Bubble rise velocity (m/s)           | 0.8          | 1.0             |
| Bubble flow rate (m <sup>3</sup> /s) | 0.0056       | 0.0056          |

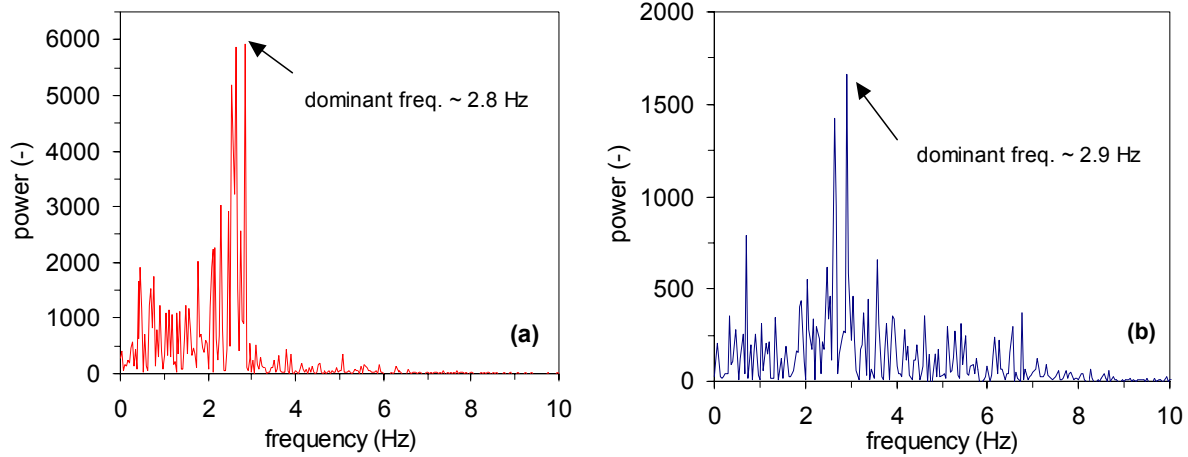


**Fig. 4. Bubble frequency spectrum estimated at  $U = 0.53$  m/s (a) Experimental (b) Mfix prediction.**

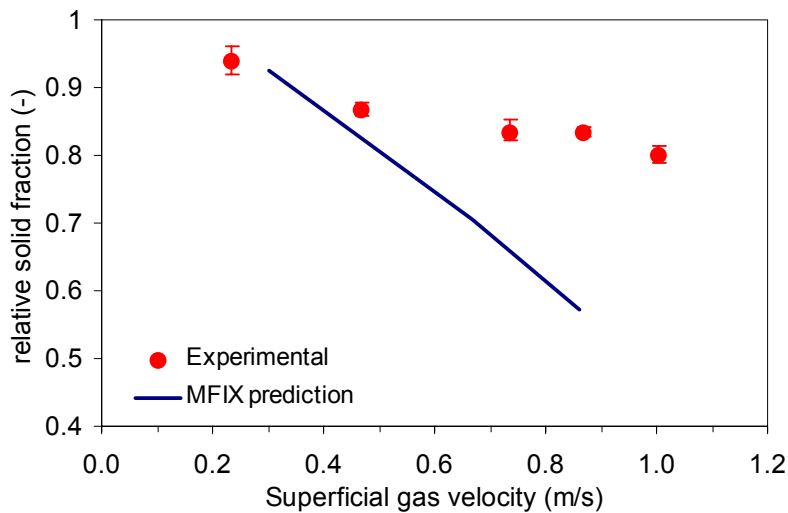


**Fig. 5. Experimental and predicted cross-sectional average solid fraction for Group B particles as function of the superficial gas velocity,  $U = 0.53$  m/s.**

The experimental and predicted solid fraction profile for Group A/B is shown in [Fig. 6](#). It is clearly seen that the model prediction is lower, which indicate an overestimated bed expansion. According to [McKeen and Pugsley \(2003\)](#), the discrepancies between the experimental and prediction as observed here is attributed to the lack of realistic formulation for the significant interparticle cohesion force (MFIx code assumes negligible cohesion force). This force leads to agglomeration and hence increasing the effective particle diameter. They found that lowering the drag force by the factor of 0.15 resulted in a better hydrodynamic match between their FCC experimental data and MFIx simulation. A reliable interparticle cohesion model, which could lead to a similar effect, is discussed [Section 5.1](#).

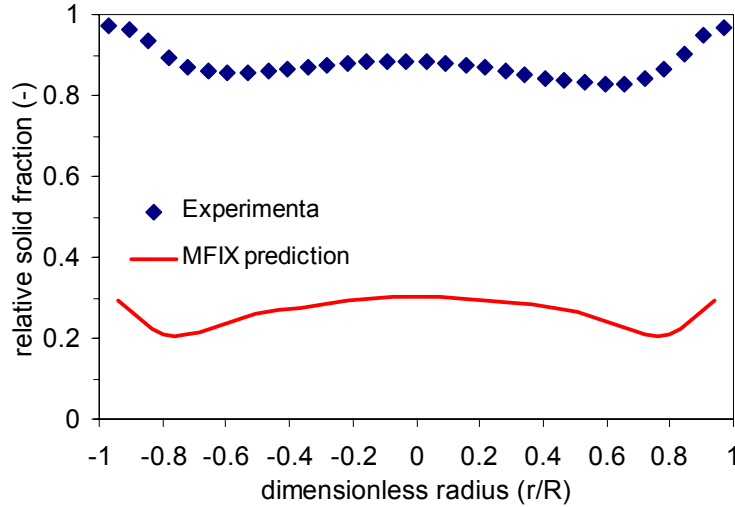


**Fig. 6. Experimental and predicted solid fraction profiles in bubbling bed of Group A/B particles at  $U = 0.23$  m/s.**

#### 4.1 Remarks:

From the above comparisons, two main conclusions can be drawn out here:

1. The MFIX code accurately predicts the various hydrodynamic features of Group B bed at high dense flow. However, the model starts to deviate showing a considerable high bed expansion as the gas velocity increase. This in part is due to the MFIX formulation, which assumes negligible frictional stress at the critical solid fraction of  $\varepsilon_s < 0.59$ . A continuous frictional model, which could lead to better predictions, is discussed in [Section 5.1](#).
2. The model fails to provide satisfactory results for Group A/B bed. This is mainly due to the MFIX neglect for the considerable effects of interparticle cohesion force. One of the ways to avoid this deficiency is to implement a realistic formulation for the interparticle cohesion force. In [Section 5.1](#), we are proposing a cohesion model, which could lead to better predictions.

#### 5. One-dimensional fully developed flow model:

A continuum fully developed gas-solid flow model has been employed here to carry out parametric sensitivity analysis. The fully developed flow equations are as follows:

$$\text{Gas momentum, x-component: } \frac{\partial \tau_{g,xy}}{\partial y} - \frac{\partial P_g}{\partial x} - \beta(u_g - u_s) = 0 \quad (12)$$

$$\text{Solid momentum, x-component: } \frac{\partial \tau_{s,xy}}{\partial y} + \frac{\partial N_{f,xy}}{\partial y} + \frac{\partial R_{c,xy}}{\partial y} + \beta(u_g - u_s) - \frac{\partial P_g}{\partial x} - \varepsilon_s \rho_s g = 0 \quad (13)$$

$$\text{Solid momentum, y-component: } \frac{\partial P_s}{\partial y} + \frac{\partial N_{f,yy}}{\partial y} + \frac{\partial R_{c,yy}}{\partial y} = 0 \quad (14)$$

The pseudo-thermal energy balance for the particle velocity fluctuation and collisions is given by:

$$\frac{\partial}{\partial y} \left( k_s \frac{\partial T}{\partial y} \right) + \tau_{s,xy} \frac{\partial u_s}{\partial y} + \gamma_s = 0 \quad (15)$$

Here  $N_f$  and  $R_c$ , given in details below, are the contribution of frictional and cohesion forces to the total solid stress respectively. Fig. 7 shows a schematic diagram for the duct orientation. For more details on other terms and boundary conditions, the reader is referred to [Ocone et al. \(1993\)](#) and [Makkawi and Ocone \(2004\)](#).

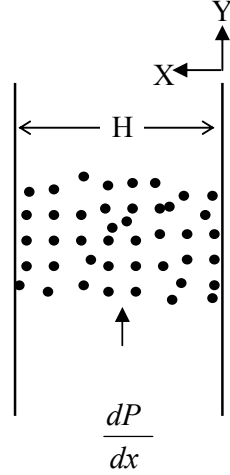


Fig. 7. Schematic of the duct orientation and flow field

### 5.1 Interparticle cohesion and frictional forces:

The widely used frictional model of [Johnson and Jackson \(1978\)](#), based on the critical state theory of soil mechanics, has a serious drawback when employed to intermediate gas-solid flow model such as bubbling bed. This model assumes zero frictional stress for solid fraction below the critical value of  $\varepsilon_{s,critical} = 0.59$ . We believe that, even at low solid fraction below the critical value, the frictional stress can still play an important rule in granular flow modelling.

Instead of the critical theory employed by MFIX, we propose here a frictional model modified from the formula of [Johnson and Jackson \(1978\)](#). Here the semi-empirical normal frictional stress is given by:

$$N_{f,yy} = Fr \frac{\varepsilon_s^{F_1}}{(\varepsilon_{s,max} - \varepsilon_s)^{F_2}} \quad (16)$$

where  $F_1$  and  $F_2$  are empirical constants given by Johnson and Jackson as 2.0 and 0.05 respectively (for glass ballotini). The parameter  $Fr$  is taken here as 0.002, this value was chosen as it reduces [Eq. 16](#) to the original formula of [Johnson and Jackson \(1978\)](#) at high solid fraction (see [Fig. 8](#)).

The frictional shear stress is given by the continuous formula of [Tardous \(2003\)](#):

$$N_{f,xy} = N_{f,yy} \sin \phi \tanh \left( \frac{a\sqrt{\pi}}{2} \right) \quad (17)$$

$$\text{were } a = \frac{2d_p}{\sqrt{2T}} \left( \frac{du_s}{dy} \right) \quad (18)$$

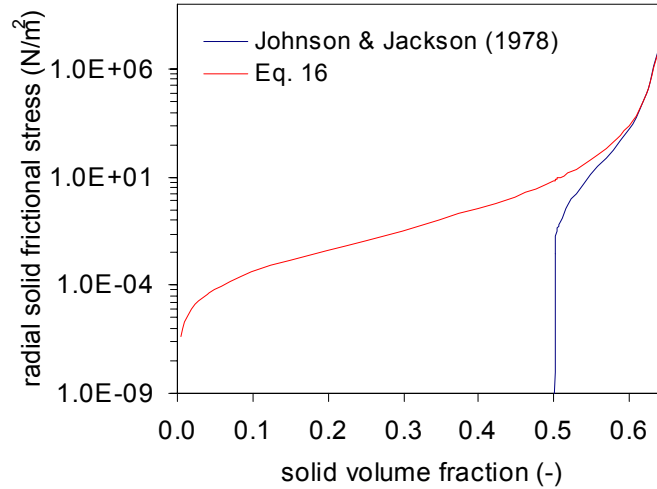


**Fig. 8. Radial solid frictional stress as function of absolute solid fraction.**

In dry granular flow, it is widely believed that the interparticle cohesion forces  $F_{ip}$  (usually referred to as van der Waals force) play a major role in defining the granular flow behaviour (Massimilla and Donsi, 1976; Molerus, 1982). According to Massimilla and Donsi (1976) the cohesion force between particles of 40 – 100  $\mu\text{m}$  diameter are exceedingly high in respect to the particle weight, and hence considered as the major factor in stabilizing the flow behaviour. For larger particles such as Group B and D, Molerous (1982) described the cohesion forces as “unimportant” and hence can be neglected.

Following Ocone et al. (2000) and Jian and Ocone (2003), the radial component of the cohesion force defined in terms of granular temperature and radial solid fraction variation is given by:

$$R_{c,yy} = C_o \frac{6\sqrt{2}F_{ip}\sqrt{T}}{u_t d} |\nabla \varepsilon_s| \quad (19)$$

where  $C_o$  is a factor used due to the uncertainty about the exact value of  $F_{ip}$ . In the literature, the values of  $F_{ip}$  for Group A/B is quite scattered. It is suggested that  $F_{ip}$  lie in the range of  $0.2 < K < 6.2$  (Molerous, 1982; Seville, 1984; Rhodes, 2001), where  $K$  is the ratio of cohesion force to the particle buoyant force. In a recent experimental study by Makkawi (2004), conducted in a bubbling bed of particle range  $d_p = 75 - 150 \mu\text{m}$ ,  $K$  was found to fall within the range of 0.2 and 0.4. In the present model we are assuming an average value of  $F_{ip} = 0.2 \times 10^{-8} \text{ N}$  (corresponding to  $K = 2$  for  $d_p = 90 \mu\text{m}$ ,  $\rho_p = 2500 \text{ kg.m}^{-3}$ ).

In obtaining the tangential cohesion force, we employed the equation of tensile force in a random cohesive packed spheres, originally proposed by Rumpf (1970) and later modified by Molerus (1982), where the tensile force is given by:

$$R_{c,xy} = R_{c,yy} \frac{\pi}{6(1 - \varepsilon_s)} \quad (20)$$

## 5.2 Results and discussion:

Fig. 9 shows the predicted solid mass flow profile of Group B particles in a vertical duct. It is clear that, neglecting the frictional stress in our model results in increasing the

mass flow. Considering a bubbling bed, this behaviour implies an increase in the material carry over and hence, a higher bed expansion. This might partly explain the poor performance of MFIX code for Geldart B bed at high gas velocity.

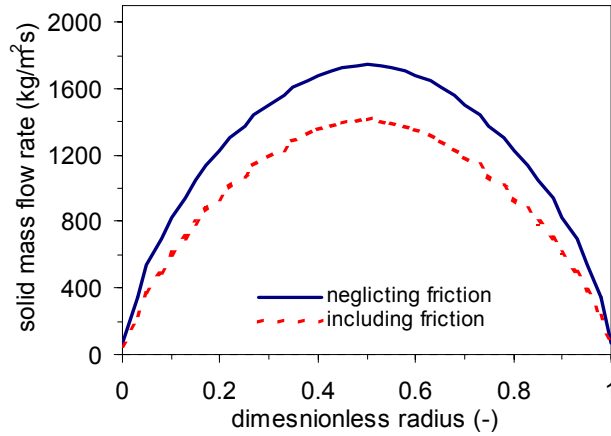


**Fig. 9. Predicted solid mass flux for Group B in a vertical duct at  $U = 9.0$  m/s.**

The corresponding solid fraction and particle velocity profiles are shown in Fig. 10. The simulation shows the classic profiles usually observed in vertical granular flow. Without the frictional stress, the predicted solid velocity and solid fraction are higher. When neglecting the frictional shear stress, the individual particles-particle contact mainly controlled by collisional effects and hence large part of the particle dynamic energy is saved towards travelling towards the top. It must be noted that, in a confined volume, such as bubbling bed, unlike the vertical duct, neglecting the frictional stress result in lowering the cross-sectional solid fraction due to the increase in material carry over.

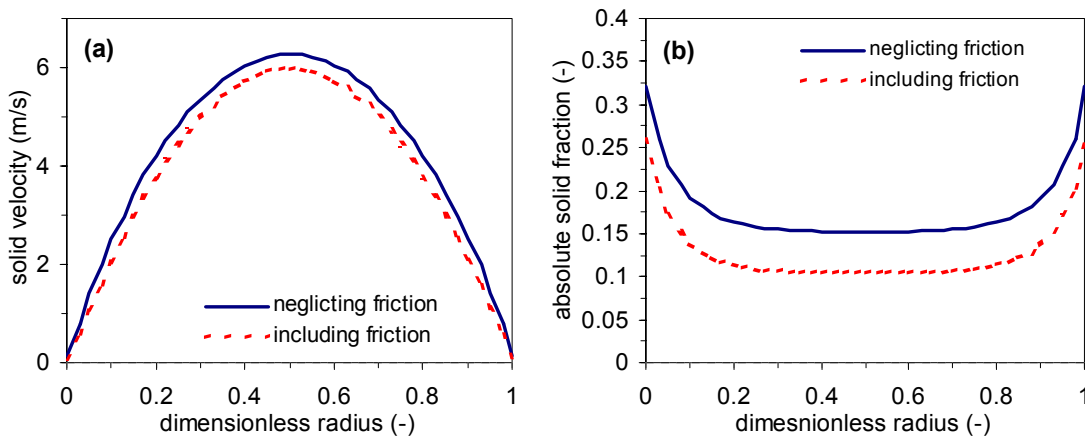


**Fig. 10. Predicted solid velocity and solid fraction for Group B in a vertical duct at  $U = 9.0$  m/s.**

We compare the computed frictional stress to the kinetic stress in Fig. 11. It is clear here that the kinetic shear stress is dominant. Nevertheless, even at this relatively low solid fraction (see Fig. 11-b), the frictional effect on the general hydrodynamic features of the flow cannot be neglected. This confirms our earlier remark noted in Section 4.1.

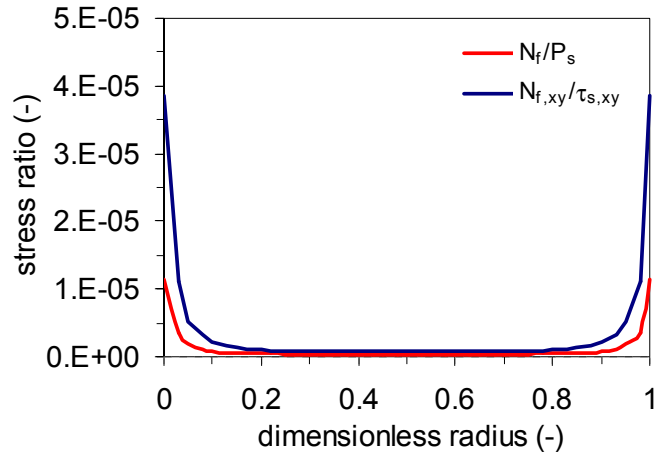


Fig. 11. Ratio of computed frictional to kinetic stress for Group B in a vertical duct at  $U = 9.0$  m/s.

Fig. 12 shows the solid mass flux and solid velocity predicted for a vertical duct of Group A/B particles at a superficial gas velocity of  $U = 5$  m/s. It is clearly seen that, as the cohesive force increases the solid mass flux decreases; it is also interesting to note the negative solid flux at high cohesive force ( $C_o = 50$ ). Similar observations are noted for the particle velocity. For a bubbling bed, the decrease in solid flux implies an equivalent decrease in the bed expansion. These observations support our earlier argument on the significant importance of interparticle cohesion force in describing Group A/B behaviour in bubbling bed or general vertical granular flow.

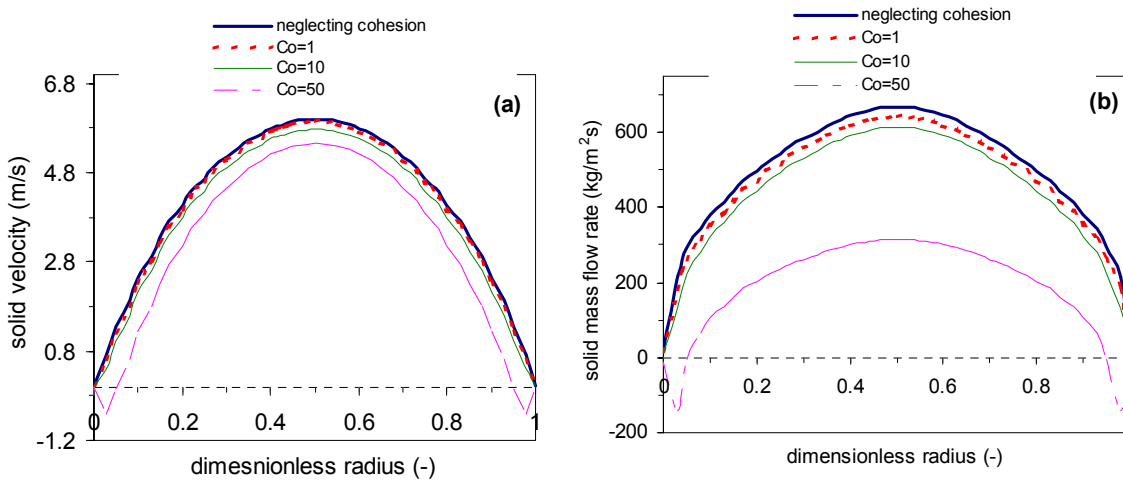
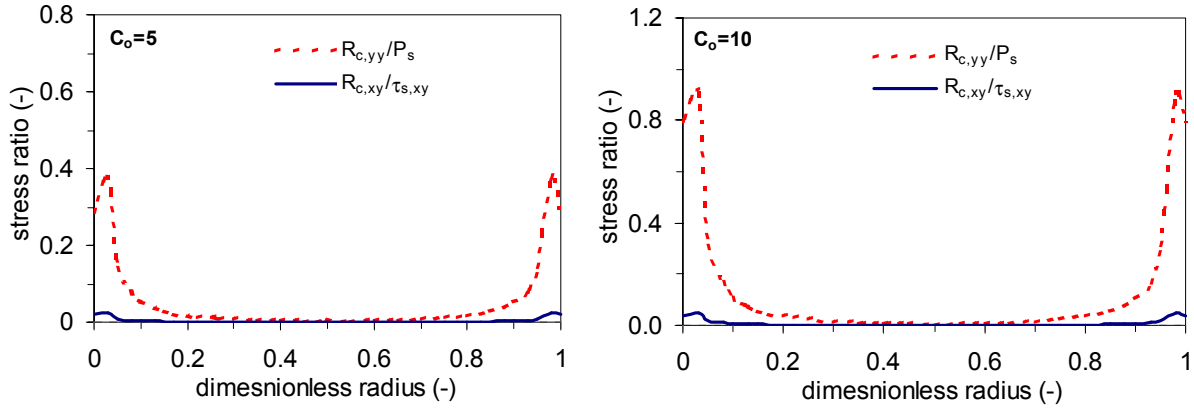


Fig. 12. Predicted solid velocity and solid mass flux for Group A/B particles in a vertical duct for different values of cohesion force at  $U = 5.0$  m/s.

Fig. 13 shows the ratio of predicted solid stress resulting from interparticle cohesion to the corresponding solid stress predicted from the classic kinetic theory. These figures indicate a dominant kinetic solid stress at the core region and a significant cohesive shear stress at the dense wall.



**Fig. 13. Predicted ratio of interparticle cohesive stress to kinetic stress for Group A/B particles in a vertical duct for different values of cohesion force at  $U = 5.0$  m/s.**

## 6. Conclusion:

Experimental ECT data of a freely bubbling bed of Group B and A/B particles has been compared to the prediction of CFD code MFIX. The model reasonably predict well the hydrodynamic features of Group B particles at low gas velocity (dense flow), however considerable bed expansion has been noticed for Group A/B and Group B at a high gas velocity. This is attributed to the fact that, in the MFIX code, the particle-particle contact force is assumed to arise from collision/viscous forces only as described by the kinetic theory, while completely neglecting cohesion and partially neglecting the frictional force at low solid fraction below the critical value of  $\varepsilon_s < 0.59$ .

A proposed interparticle cohesion and frictional force terms has been tested in a continuum fully developed flow model to investigate their effect on the general hydrodynamic features of vertical duct flow. It is observed that both terms has direct effect on lowering the material carryover, which implies a reduced bed expansion in freely bubbling column. The parametric analysis shows that the cohesion in Group A/B and frictional force in Group B are significantly high when compared to the kinetic stress, and hence it can play a major rule in describing the hydrodynamic features of the flow. Work is still in progress to incorporate a realistic cohesion and frictional terms in a MFIX code.

## Nomenclature

|                |   |
|----------------|---|
| $a$            | parameter defined in Eqs. 17 and 18 (-)                                       |
| $\overline{D}$ | strain rate tensor ( $s^{-1}$ )   |
| $d_p$          | particle diameter (m)   |
| $e_p, e_w$     | Particle-particle and particle-wall restitution coefficients respectively (-) |
| $Fr, F_1, F_2$ | parameters defined in Eq. 16  |
| $F_p$          | interparticle cohesion force (N)  |
| $g$            | gravity acceleration constant ( $ms^{-2}$ )                                   |
| $H$            | duct width (m)  |
| $I_{2D}$       | second deviator of strain rate tensor ( $s^{-2}$ )                            |
| $K$            | ratio of interparticle cohesion force to particle weight force (-)            |
| $k_s$          | effective thermal conductivity of particles ( $kgm^{-1}s^{-1}$ )              |

|            |  |
|------------|--|
| $N_f$      | frictional stress (Nm <sup>-2</sup> )  |
| $n_b$      | total number of bubbles in a specific time interval (-)  |
| $P$        | pressure (-)   |
| $p$        | relative solid fraction (-)  |
| $Q_b, q_b$ | instantaneous and time averaged volumetric bubble flow rate respectively (m <sup>3</sup> s <sup>-1</sup> ) |
| $R_c$      | interparticle cohesion stress (Nm <sup>-2</sup> )  |
| $Re_p$     | particle Reynolds number in terms of interstitial velocity, $= \rho_g (u_g - u_s) d_p / \mu_g$ , (-)       |
| $T$        | granular temperature (m <sup>2</sup> .s <sup>-2</sup> )  |
| $t$        | time (s)   |
| $U$        | superficial gas velocity (ms <sup>-1</sup> )   |
| $u$        | velocity vector (N/m <sup>2</sup> )  |
| $U_b, u_b$ | time averages and instantaneous bubble rise velocity (ms <sup>-1</sup> )                                   |
| $u_t$      | terminal velocity of single isolated particle (m/s)  |
| $x$        | axial coordinate   |
| $y$        | radial coordinate  |

### **Greek symbols**

|               |   |
|---------------|---|
| $\varepsilon$ | absolute volume fraction (-)                          |
| $\rho$        | density (kg.m <sup>-3</sup> )                         |
| $\tau$        | viscous shear stress (N.m <sup>-2</sup> )             |
| $\gamma_s$    | dissipation of granular energy (kgm <sup>-3</sup> s)  |
| $\beta$       | gas-solid interphase drag coefficient (-)             |
| $\phi$        | angle of internal friction for the particle (degrees) |

### **Subscripts**

|          |   |
|----------|---|
| $g$      | gas phase   |
| $s$      | solid phase   |
| $xy, yy$ | axial and radial coordinate components respectively |

### **References**

- Coulomb, C. A, 1776, In Wachem, B. G., Schouten, J. C., van den Bleek, C. M., 2001. Comparative analysis of CFD models of dense gas-solid systems. AICHE Journal 47, 1035-1051.
- Ferschneider, G., and Mega, P., 1996. In McKeen, T., and Pugsley, T., 2003. Simulation and experimental validation of freely bubbling bed of FCC catalyst. Powder Technology 129, 139-152
- Gibilaro, L. G., Felice, R. Di., Waldram, S. P., 1985. Generalized friction factor and drag coefficient correlation for fluid-particle interactions. Chemical Engineering Science 40 (10), 1817-1823.
- Huilin, L., Yurong H., Wentie, L., Ding, J., Gidaspow, D., Bouillard, J., 2004. Computer simulations of gas-solid flow in spouted beds using kinetic-frictional stress model of granular flow. Chemical Engineering Science 59. 865-878.
- Jenike, A. W., 1978. A theory of flow of particulate solids in converging channels based on a conical yield function. Powder Technology 50, 229-236.
- Jian, H. and Ocone, R., 2003. Modelling the hydrodynamics of gas-solid suspension in downers. Powder Technology 138. 73-81.

Johnson, P. C., and Jackson, R., 1987. Frictional-collisional constitutive relations for granular materials, with application to plane shearing. *Journal of Fluid Mechanics* 176, 67-93.

Lun, C. K., Savage, S. B., Jeffrey, D. J., 1984. Kinetic theories for granular flow: inelastic particles in coquette flow and slightly inelastic particles in a general flowfield. *Journal of Fluid Mechanics* 140, 223-256.

Makkawi, Y. T., 2004. Investigation of dry and semi-wet fluidized bed hydrodynamics utilizing twin-pane electrical capacitance tomography. PhD thesis, Heriot-Watt university, UK.

Makkawi, Y. T. and Ocone, R., 2004. Hydrodynamic simulation of gas-solid flow in inclined duct using kinetic-frictional stress models. AIChE meeting, Nov 7-12, Austin TX, US. Submitted.

Makkawi, Y. T., and Wright, P. C., 2002. Optimization of data acquisition rate and experiment span for reliable ECT measurement in fluidized beds. *Measurement Science and Technology* 13 (12), 1831-1841

Massimilla, L. and Donsi, G., 1976. Cohesive force between particles of fluid bed catalyst. *Powder Technology* 15, 253-260.

McKeen, T., and Pugsley, T., 2003. Simulation and experimental validation of freely bubbling bed of FCC catalyst. *Powder Technology* 129, 139-152.

Molwrous, O., 1982. Interperation of Geldart type A, B, C and D powders by taking into account interparticle forces. *Powder Technology* 33, 81-87.

Ocone, R., Sundaresan, S., Jackson, R., 1993. Gas-particle flow in a duct of arbitrary inclination with particle-particle interaction. *Fluid Mechanics and Transport Phenomena* 39, 1261-1271.

Rumpf, H., 1970. Zur Theorie der Zugfestigkeit an Kontakt-punkten, *Chem Ing. Tech.*, 42. 538.

Seville, J. P., Willett, C. D., Knight, P. C., 2000. Interparticle forces in fluidization; a review. *Powder Technology* 113, 261-268.

Syamlal, M., Rogers, W. A., O'Brien, T. J. 1993. MFIx documentation and theory guide, DOE/METC94/1004, NTIS/DE94000087. Electronically available at <http://www.mfix.org>.

Tardos, G. I, McNamara, S., Talu, I., 2003. Slow and intermediate flow of frictional bulk powder in the coquette geometry. *Powder Technology* 131, 23-39.